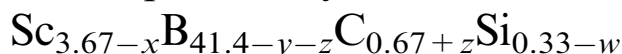


# A novel boron-rich quaternary scandium borocarbosilicide



Takaho Tanaka,\* Akiji Yamamoto, and Akira Sato

National Institute for Materials Science, Advanced Materials Laboratory, Namiki 1-1, Tsukuba, Ibaraki 305-0044, Japan

Received 4 September 2002; accepted 3 February 2003

## Abstract

A novel quaternary scandium borocarbosilicide  $\text{Sc}_{3.67-x}\text{B}_{41.4-y-z}\text{C}_{0.67+z}\text{Si}_{0.33-w}$  was found. Single crystallites were obtained as an intergrowth phase in the float-zoned single crystal of  $\text{Sc}_{0.83-x}\text{B}_{10.0-y}\text{C}_{0.17+y}\text{Si}_{0.083-z}$  that has a face-centered cubic crystal structure. Single crystal structure analysis revealed that the compound has a hexagonal structure with lattice constants  $a = b = 1.43055(8)$  nm and  $c = 2.37477(13)$  nm and space group  $P\bar{6}m2$  (No. 187). The crystal composition calculated from the structure analysis for the crystal with  $x = 0.52$ ,  $y = 1.42$ ,  $z = 1.17$ , and  $w = 0.02$  was  $\text{ScB}_{12.3}\text{C}_{0.58}\text{Si}_{0.10}$  and that agreed rather well with the composition of  $\text{ScB}_{11.5}\text{C}_{0.61}\text{Si}_{0.04}$  measured by EPMA. In the crystal structure that is a new structure type of boron-rich borides, there are 79 structurally independent atomic sites, 69 boron and/or carbon sites, two silicon sites and eight scandium sites. Boron and carbon form seven structurally independent  $\text{B}_{12}$  icosahedra, one  $\text{B}_9$  polyhedron, one  $\text{B}_{10}$  polyhedron, one irregularly shaped  $\text{B}_{16}$  polyhedron in which only 10.7 boron atoms are available because of partial occupancies and 10 bridging sites. All polyhedron units and bridging site atoms interconnect each other forming a three-dimensional boron framework structure. Sc atoms reside in the open spaces in the boron framework structure.

© 2003 Elsevier Inc. All rights reserved.

**Keywords:**  $\text{Sc}_{3.67-x}\text{B}_{41.4-y-z}\text{C}_{0.67+z}\text{Si}_{0.33-w}$ ; Scandium borocarbosilicide; Single crystal structure analysis; Hexagonal structure;  $\text{B}_{12}$  icosahedron compound

## 1. Introduction

In the last decade one of the authors (T. T.) have searched for new boron-rich rare earth borides that can replace  $\text{YB}_{66}$ .  $\text{YB}_{66}$  single crystal is useful as a soft X-ray monochromator for dispersing synchrotron radiation from 1 to 2 keV energy region [1, 2]. Although  $\text{YB}_{66}$  satisfies most of the material requirements for the soft X-ray monochromator use, one exceptional property is its amorphous like low thermal conductivity, which makes it difficult to use the  $\text{YB}_{66}$  monochromator extensively on brighter insertion device beam lines.

Only boron-rich Sc or Y borides can be a candidate because other rare earth elements have  $M$  absorption edges in the required energy range of 1–2 keV. According to this restriction boron-rich Sc borides have been extensively searched [3] and previously we reported the floating zone crystal growth and the structure analysis of

$\text{Sc}_{0.83-x}\text{B}_{10.0-y}\text{C}_{0.17+y}\text{Si}_{0.083-z}$  ( $x = 0.030$ ,  $y = 0.36$ ,  $z = 0.026$ ,  $\text{ScB}_{12.0}\text{C}_{0.65}\text{Si}_{0.071}$ ), which has a face-centered cubic crystal structure [4]. During the crystal growth experiments we found that two new phases whose compositions were very close to the cubic phase appeared as inclusions. Sizable single crystals of one of the two phases could be grown by the floating zone method although the phase appeared only at the initial stage of the float zone pass. It could be identified as an orthorhombic phase with the measured composition of  $\text{ScB}_{12.9}\text{C}_{0.72}\text{Si}_{0.004}$ . The details of the structure analysis are reported elsewhere [5].

On the other hand, single crystal growth of another phase is not successful up to now. However, crystallites of the phase with several mm sizes appeared on the surface of the zone passed rod during the crystal growth of the cubic phase, especially at the initial stage of the zone pass. One crystallite could be isolated from the rod, and sent to density measurement, chemical composition analysis by EPMA and structure analysis. The structure analysis revealed that the phase has a hexagonal

\*Corresponding author. Fax: +81-298-52-7449.

E-mail address: [tanaka.takaho@nims.go.jp](mailto:tanaka.takaho@nims.go.jp) (T. Tanaka).

structure with lattice constants  $a = b = 1.43055(8)$  nm and  $c = 2.37477(13)$  nm and space group  $P\bar{6}m2$  (No. 187).

In this paper the structure analysis of the hexagonal phase is presented.

## 2. Results and discussion

Experimental details of crystal growth and EPMA measurement were given previously [4, 5]. A single crystal specimen for single crystal XRD data collection could be obtained by cracking a part of the grown crystallite. Before cracking the density of the crystallite was measured by standard buoyancy method using hexachloro-1, 3-butadiene as a buoyancy medium. After cracking the remaining part was sent to EPMA measurement. The obtained Sc, B, C and Si contents were  $25.2 \pm 0.1$ ,  $69.9 \pm 1.2$ ,  $4.1 \pm 0.1$  and  $0.6 \pm 0.1$  wt%, respectively and sum of each mean value is 99.8 wt%. The normalized chemical composition is  $\text{ScB}_{11.5}\text{C}_{0.61}\text{Si}_{0.04}$ .

The single crystal X-ray diffraction data were collected in two ways: (1) an imaging plate Weissenberg camera (Mac Science Co., Japan) with graphite monochromated  $\text{NbK}\alpha$  radiation and (2) an Enraf-Nonius CAD4 automatic 4-circle diffractometer with graphite monochromated  $\text{MoK}\alpha$  radiation. The crystal quality was checked by Weissenberg camera prior to the single crystal XRD data collection. From the single crystal XRD data collected by the imaging plate Weissenberg camera we could reject a possibility of twinning in the specimen. Although the structure refinements using both data sets gave almost same results, the latter gave slightly better  $R1$  and  $R2$  values, thus this will be used for discussion hereafter. The crystal data and the 4-circle intensity measurement data are given in Table 1. The intensity data were corrected for Lorentz and polarization effects. The absorption correction applied to the collected data was empirically based on  $\Psi$ -scans.

### 2.1. Structure analysis

An initial solution was obtained by SIR92 [6] according to the space group  $P\bar{6}m2$  (No. 187) and the program SHELXL-97 [7] was used for refinement. The direct method gave 79 atomic positions in which eight Sc sites, two Si sites, eight C sites and 61 B sites were assigned. The refinement using the assignment gave  $R1$  value of 6.1% with 266 parameters for 2851 independent reflections [ $F_o > 4\sigma(F_o)$ ]. Visualization of the crystal structure using the graphic program CrystalMaker [8] immediately showed a three-dimensional boron framework composed of interconnected  $\text{B}_{12}$  icosahedra, a  $\text{B}_9$  polyhedron, a  $\text{B}_{10}$  polyhedron, an irregularly shaped

Table 1  
Crystallographic and data collection parameters

Crystal composition	$\text{ScB}_{11.7}\text{C}_{0.6}\text{Si}_{0.04}$ (obtained by EPMA measurement)
Crystal system	Hexagonal
Space group	$P\bar{6}m2$ (No. 187)
Lattice constant (nm)	$a = 1.43055(8)$ , $c = 2.37477(13)$
Unit cell volume ( $\text{nm}^3$ )	4.209
Empirical formula	$\text{Sc}_{3.67-x}\text{B}_{41.4-y-z}\text{C}_{0.67+z}\text{Si}_{0.33-w}$ ( $x = 0.52$ , $y = 1.42$ , $z = 1.17$ , $w = 0.02$ ) ( $\text{ScB}_{12.3}\text{C}_{0.58}\text{Si}_{0.10}$ )
Z	12
$D_x$ ( $\text{g}/\text{cm}^3$ )	2.804
$D_m$ ( $\text{g}/\text{cm}^3$ )	2.832
$\mu$ for $\text{MoK}\alpha$ ( $\text{cm}^{-1}$ )	15.77
Crystal dimensions (mm)	$0.20(001) \times 0.18(100) \times 0.18(120)$
Reflection measured	$0 \leq h \leq 23$ , $0 \leq k \leq 23$ , $-22 \leq l \leq 38$
$2\theta$ max.	$45^\circ$
Structure refinement program	SHELXL97
$R1$	0.047 ( $F_o > 4\sigma(F_o)$ , for 2851 $F_o$ ), 0.068 (all $F_o$ , for 3619 $F_o$ )
$wR2$	0.123 ( $F^2$ )
Number of variables	286
Number of independent atoms	79

polyhedron and bridging boron, carbon and silicon sites.

Careful examination of both bond distances and temperature factors required us to reassign one Sc site to a Si site and one Si site to a Sc site. Thus total number of both Sc and Si sites was kept the same. Five C sites were turned to B sites and one B site was turned to a C site. Moreover B and C mixed occupancy was applied to six B or C sites. Finally 62 B sites, two C sites and six B/C mixed occupancy sites were counted. Since six B sites have too close neighbor sites, partial occupancy was applied to the sites. Partial occupancy was applied to one of two Si sites and all Sc sites also. The final refinement gave  $R1$  value of 4.7% with 286 parameters for 2851 independent reflections [ $F_o > 4\sigma(F_o)$ ] and 6.8% for all 3619 independent reflections. The final atomic coordinates, occupancy factors and temperature factors are listed in Table 2.

Anomalous large temperature factors of quite a lot of boron atom sites with full occupancy could be observed. However, this should not be understood as a sign of the imperfect description of the crystal structure. In the crystal structure such boron atom sites are bonded to the boron site with partial occupancy. A slight shift of the sites would be caused depending on the absence and existence of the partial occupancy site. Such shifts are not so large as those to be expressed as a split site but appear as seemingly large temperature factors of those sites.

This compound has some amount of homogeneity region, thus it can be written as  $\text{Sc}_{3.67-x}\text{B}_{41.4-y-z}$

Table 2  
Final atomic coordinates, occupancy factors and temperature factors

Atom	Site	x	y	z	Occupancy	$U(\text{\AA}^2 \times 10^3)$
B1	6n	0.8073(5)	0.4037(3)	0.0812(3)	1.0	6.8(10)
B2	6n	0.0650(5)	0.5325(2)	0.1400(2)	1.0	6.0(9)
B3	6n	0.9269(5)	0.4634(2)	0.0374(2)	1.0	4.4(9)
B4	6n	0.9436(5)	0.4718(3)	0.1852(3)	1.0	6.9(10)
B5	12o	0.8402(4)	0.3568(3)	0.1453(2)	1.0	7.1(7)
B6	12o	0.9843(3)	0.3894(3)	0.1412(2)	1.0	6.0(7)
B7	12o	0.0316(3)	0.4545(3)	0.0749(2)	1.0	5.7(7)
B8	12o	0.8989(4)	0.3458(4)	0.0781(2)	1.0	7.1(7)
B9	6n	0.1969(5)	0.5984(3)	0.1645(3)	1.0	8.0(10)
B10	6n	0.2446(5)	0.6223(3)	0.2375(3)	1.0	8.2(11)
B11	6n	0.2920(2)	0.5839(5)	0.1205(2)	1.0	5.3(9)
B12	6n	0.2647(3)	0.5294(5)	0.1913(2)	1.0	5.7(9)
B13	6n	−0.2671(59)	0.2671(5)	0.3155(3)	1.0	8.3(10)
B14	6n	0.8217(3)	0.1784(3)	0.3748(3)	1.0	12.2(11)
B15	6n	0.7742(3)	0.2258(3)	0.2397(2)	1.0	6.1(9)
B16	12o	0.7213(4)	0.0679(4)	0.3317(2)	1.0	10.4(8)
B17	12o	0.8736(4)	0.3358(4)	0.2828(2)	1.0	8.9(7)
B18	6n	0.7304(3)	0.2697(3)	0.2990(3)	1.0	12.0(12)
B19	12o	0.9027(4)	0.2288(4)	0.2599(2)	1.0	8.7(7)
B20	12o	0.8261(5)	0.3023(5)	0.3556(2)	1.0	17.5(10)
B/C21	6n	−0.0808(5)	0.0808(5)	0.3880(2)	B/C=0.55/0.45	6.7(9)
B22	6n	0.0675(3)	−0.0675(3)	0.3478(2)	1.0	6.8(10)
B23	6n	0.9185(5)	−0.0408(2)	0.2783(2)	1.0	5.8(9)
B24	6n	0.9333(3)	−0.1334(5)	0.3221(2)	1.0	6.0(10)
B/C25	6l	0.3352(5)	0.5516(5)	0.0	B/C=0.55/0.45	6.8(10)
B26	12o	0.3193(3)	0.4403(4)	0.0374(2)	1.0	5.8(7)
B27	6n	0.1829(2)	0.3658(5)	0.0603(2)	1.0	4.2(9)
B28	6l	0.2238(5)	0.3231(5)	0.0	1.0	5.4(9)
B29	6n	0.2548(3)	0.5096(5)	0.0612(3)	1.0	6.0(9)
B30	12o	0.1777(4)	0.4848(4)	0.3452(2)	1.0	8.9(7)
B31	6n	0.2658(3)	0.5316(6)	0.5902(3)	1.0	11.8(11)
B32	6n	0.1323(3)	0.2646(5)	0.3660(3)	1.0	7.8(10)
B33	6n	0.1854(3)	0.3708(5)	0.3161(3)	1.0	7.7(10)
B34	12o	0.0915(4)	0.3082(4)	0.4271(2)	1.0	8.7(7)
B35	12o	0.0677(4)	0.3465(4)	0.3582(2)	1.0	9.6(7)
B36	12o	0.1183(5)	0.4431(5)	0.4173(2)	1.0	15.6(9)
B37	6n	0.2096(3)	0.7905(3)	0.4609(3)	1.0	9.7(11)
B/C38	6m	0.0027(5)	0.1179(5)	0.5	B/C=0.65/0.35	6.8(9)
B39	6m	0.7666(5)	0.1089(5)	0.5	1.0	6.9(10)
B40	12o	0.9869(4)	0.2146(4)	0.4628(2)	1.0	7.4(7)
B/C41	6n	0.9211(2)	−0.1578(5)	0.4421(2)	B/C=0.45/0.55	7.1(9)
B42	6n	0.8514(3)	0.1486(3)	0.4387(3)	1.0	6.7(9)
B43	6l	0.2387(5)	0.2133(5)	0.0	1.0	6.4(10)
B44	12o	0.8843(3)	0.2383(3)	−0.0392(2)	1.0	6.0(7)
B45	3j	0.1431(7)	0.0716(3)	0.0	1.0	3.3(13)
B46	6n	0.2359(5)	0.1180(2)	−0.0579(2)	1.0	4.6(9)
B47	6n	0.1969(3)	0.3938(6)	0.1835(3)	1.0	12.4(12)
B48	6n	0.1543(3)	0.3086(5)	0.1262(2)	1.0	6.0(10)
B49	12o	0.0178(4)	0.2465(4)	0.2240(2)	1.0	9.9(8)
B50	6n	0.0872(2)	0.1745(5)	0.2267(2)	1.0	6.6(9)
B51	12o	0.0563(4)	0.3250(4)	0.1626(2)	1.0	8.7(7)
B52	6n	0.1530(3)	0.3060(6)	0.2517(3)	1.0	13.3(12)
B53	12o	0.1623(3)	0.1884(3)	0.1601(2)	1.0	5.9(7)
B54	6m	0.4507(8)	0.3567(8)	0.5	1.0	27.0(18)
B55	12o	0.4300(9)	0.9827(9)	0.4547(4)	0.87	43.8(29)
B56	6n	0.5907(5)	0.4093(5)	0.3925(5)	0.66	17.7(32)
B57	6n	0.8050(13)	0.4025(7)	0.4762(6)	0.51	16.9(40)
B58	12o	0.5007(9)	0.3781(9)	0.4206(5)	0.44	12.2(28)
B59	6n	0.8881(16)	0.4440(8)	0.4595(8)	0.55	30.9(53)
C60	2i	0.6667	0.3333	−0.7126(5)	1.0	15.9(21)
B61	1a	0.0	0.0	0.0	1.0	10.5(27)
B62	6n	0.1877(5)	0.5939(3)	0.3066(3)	1.0	9.4(11)

Table 2 (continued)

Atom	Site	<i>x</i>	<i>y</i>	<i>z</i>	Occupancy	$U(\text{\AA}^2 \times 10^3)$
C63	6 <i>n</i>	0.7421(2)	0.2579(2)	0.1798(2)	1.0	8.6(9)
B/C64	6 <i>n</i>	0.9344(5)	0.4672(2)	0.2578(2)	B/C=0.57/0.43	6.2(10)
B65	6 <i>n</i>	0.9172(3)	0.0828(3)	0.1237(3)	1.0	6.1(9)
B66	1 <i>f</i>	0.6667	0.3333	0.5	1.0	43.4(68)
B/C67	2 <i>h</i>	0.3333	0.6667	0.5774(5)	B/C=0.71/0.29	10.5(22)
B68	2 <i>i</i>	0.6667	0.3333	0.0639(4)	1.0	5.0(16)
B69	2 <i>h</i>	0.3333	0.6667	0.3006(8)	0.49	0.0(44)
Si1	2 <i>i</i>	0.6667	0.3333	0.3919(2)	0.87	30.7(16)
Si2	2 <i>i</i>	0.6667	0.3333	0.2078(1)	1.0	5.0(5)
Sc1	2 <i>g</i>	0.0	0.0	0.17777(8)	0.98	5.5(4) <sup>a</sup>
Sc2	3 <i>j</i>	0.74237(6)	−0.74237(6)	0.0	0.95	7.0(4) <sup>a</sup>
Sc3	6 <i>n</i>	0.07873(4)	−0.07873(4)	−0.06563(4)	0.96	4.5(2) <sup>a</sup>
Sc4	12 <i>o</i>	0.07726(8)	0.43056(8)	0.24776(3)	0.87	9.4(2) <sup>a</sup>
Sc5	6 <i>n</i>	0.82732(5)	−0.82732(5)	0.14302(6)	0.96	19.5(4) <sup>a</sup>
Sc6	6 <i>n</i>	0.50007(6)	−0.50007(6)	0.35580(6)	0.91	14.4(3) <sup>a</sup>
Sc7	3 <i>k</i>	0.40577(10)	−0.40577(10)	0.5	0.88	31.1(9) <sup>a</sup>
Sc8	6 <i>n</i>	0.74848(9)	0.25152(9)	0.45210(9)	0.49	6.3(5) <sup>a</sup>
	<i>U</i> 11	<i>U</i> 22	<i>U</i> 33	<i>U</i> 23	<i>U</i> 13	<i>U</i> 12
Sc1	4.7(5)	4.7(5)	7.1(8)	0.0	0.0	2.4(3)
Sc2	8.5(6)	8.5(6)	7.3(6)	0.0	0.0	6.8(6)
Sc3	4.6(3)	4.6(3)	4.1(4)	−0.2(2)	0.2(2)	2.1(4)
Sc4	7.0(4)	8.5(4)	11.6(3)	−4.2(3)	−1.4(3)	3.1(2)
Sc5	26.9(6)	26.9(6)	18.2(6)	−2.8(2)	2.8(2)	23.6(7)
Sc6	13.6(5)	13.6(5)	16.4(6)	0.1(2)	−0.1(2)	7.1(5)
Sc7	15.0(9)	15.0(9)	66.7(21)	0.0	0.0	10.3(9)
Sc8	4.9(7)	4.9(7)	7.9(9)	−0.8(3)	0.8(3)	1.7(7)

<sup>a</sup> For Sc sites anisotropic thermal factors are applied and  $U_{\text{eq}}$  (one-third of the trace of the orthogonized  $U_{ij}$  tensor) is denoted in these columns.

$\text{C}_{0.67+z}\text{Si}_{0.33-w}$ , where the number in the suffix of the elements is the total number of sites divided by the maximum multiplicity of 12. *x*, *y* and *w* indicate defects of Sc, B and Si sites, respectively, and *z* indicates degree of mixed occupancy between B and C. Width of the homogeneity region of this compound was not determined in this investigation. For the present crystal the values are  $x = 0.52$ ,  $y = 1.42$ ,  $z = 1.17$  and  $w = 0.02$ . Thus the composition normalized for Sc is  $\text{ScB}_{12.3}\text{C}_{0.58}\text{Si}_{0.10}$ , which agrees rather well with the composition  $\text{ScB}_{11.5}\text{C}_{0.61}\text{Si}_{0.04}$  measured by EPMA. For the present crystal the measured density  $2.832 \text{ g/cm}^3$  is higher than the calculated one,  $2.804 \text{ g/cm}^3$ . Both the cubic and orthorhombic phases have lower measured density than the present hexagonal phase so that the high value of the measured density could not be attributed to the inclusion of other two phases. The same phenomena were also observed for previous both cubic and orthorhombic phases. Probably the Sc site occupancies are somehow underestimated due to the use of neutral Sc atom for the refinement, although rare earth elements in boron-rich borides are expected to be in an ionized state. In fact, on the structure refinement of  $\text{YB}_{62}$  and  $\text{YB}_{56}$  occupancy of the Y site increased with an increase in charge number of Y and the atomic ratio approached  $\text{YB}_{62}$  or  $\text{YB}_{56}$  determined by chemical analysis [9].

However, such treatment is rather time consuming and is not the subject matter of the present paper. Instead, a simple assumption was tried; if the Sc site occupancies are increased from 3.15 to 3.3 in the empirical formula by adjusting the  $[\text{B} + \text{C}]/[\text{Sc}]$  ratio to that obtained by EPMA measurement, the calculated density would become  $2.836 \text{ g/cm}^3$  which almost coincides with the measured density.

In the crystal structure there are seven structurally independent icosahedra I1–I7 that are formed by B1–B8, B9–B12, B13–B20, B/C21–B24, B/C25–B29, B30–B37 and B/C38–B42, as grouped in Table 2. B43–B46 forms the  $\text{B}_9$  polyhedron and B47–B53 forms the  $\text{B}_{10}$  polyhedron. B54–B59 forms the irregularly shaped  $\text{B}_{16}$  polyhedron in which only 10.7 boron atoms are available because most of the sites are too close to be occupied simultaneously. Ten bridging sites from C60 to B69 interconnect polyhedron units or other bridging site to form a three-dimensional boron framework.

The interatomic B–B and/or B–C distances are summarized in Table 3. Seven icosahedra can be classified into two, a large one and a small one: the former groups I1, I2, I3 and I6 which consist of only boron atoms have the average intraicoahedral bond distances of 1.821, 1.827, 1.824 and 1.830 Å, respectively,

Table 3  
Interatomic distances (Å)

B–B bond lengths within B <sub>12</sub> icosahedra					
<i>Icosahedron I1</i>					
B1–B3	1.811(8)	B3–B7	1.802(6)	B5–B6	1.875(6)
B1–B5	1.817(7)	B3–B8	1.804(5)	B6–B7	1.782(6)
B1–B8	1.868(6)	B4–B5	1.832(7)	B6–B8	1.834(6)
B2–B6	1.778(5)	B4–B6	1.873(6)	B7–B8	1.754(6)
B2–B7	1.827(6)	B5–B5	1.810(9)	B7–B7	1.755(8)
B2–B4	1.848(8)	B5–B8	1.846(6)		
<i>Icosahedron I2</i>					
B9–B11	1.807(6)	B9–B10	1.831(9)	B10–B10	1.904(11)
B9–B12	1.812(5)	B10–B12	1.853(6)	B11–B11	1.775(10)
				B11–B12	1.812(8)
<i>Icosahedron I3</i>					
B13–B19	1.778(7)	B15–B17	1.820(6)	B17–B20	1.830(7)
B13–B14	1.794(9)	B15–B19	1.880(7)	B17–B19	1.856(7)
B13–B16	1.842(6)	B16–B20	1.802(7)	B18–B20	1.805(8)
B14–B20	1.801(8)	B16–B19	1.814(6)	B19–B19	1.882(10)
B14–B16	1.828(6)	B16–B17	1.843(6)	B20–B20	1.837(11)
B15–B18	1.781(9)	B17–B18	1.818(6)		
<i>Icosahedron I4</i>					
B/C21–B24	1.696(8)	B22–B24	1.771(5)	B23–B24	1.779(6)
B/C21–B/C21	1.735(11)	B22–B23	1.778(8)		
B/C21–B22	1.743(6)	B23–B23	1.750(10)		
<i>Icosahedron I5</i>					
B/C25–B/C25	1.701(12)	B26–B26	1.777(8)	B27–B28	1.768(6)
B/C25–B26	1.736(7)	B26–B27	1.778(5)	B27–B29	1.782(9)
B/C25–B29	1.762(6)	B26–B28	1.782(7)	B28–B28	1.782(12)
B26–B29	1.753(6)				
<i>Icosahedron I6</i>					
B30–B33	1.825(7)	B31–B36	1.848(7)	B34–B34	1.792(9)
B30–B35	1.836(7)	B32–B33	1.770(9)	B34–B35	1.811(6)
B30–B30	1.851(9)	B22–B34	1.790(7)	B34–B37	1.826(7)
B30–B36	1.873(7)	B32–B35	1.829(6)	B35–B36	1.845(7)
B30–B31	1.884(7)	B33–B35	1.836(6)	B36–B37	1.827(7)
B31–B37	1.847(10)	B34–B36	1.784(7)		
<i>Icosahedron I7</i>					
B/C38–B/C41	1.707(6)	B39–B40	1.761(7)	B40–B/C41	1.752(6)
B/C38–B/C38	1.725(12)	B39–B39	1.782(12)	B40–B40	1.766(8)
B/C38–B40	1.747(7)	B39–B42	1.796(6)	B40–B42	1.775(6)
				B/C41–B42	1.729(8)
B–B bond lengths within the B <sub>9</sub> polyhedron					
B43–B44	1.768(7)	B44–B44	1.755(8)	B45–B46	1.793(8)
B43–B45	1.792(9)	B44–B46	1.763(7)		
B43–B46	1.924(6)	B44–B44	1.862(8)		
B–B bond lengths within the B <sub>10</sub> polyhedron					
B47–B48	1.722(9)	B49–B51	1.751(6)	B50–B52	1.734(9)
B47–B51	1.811(6)	B49–B50	1.753(6)	B50–B53	1.866(6)
B47–B52	1.951(10)	B49–B53	1.762(6)	B51–B53	1.780(6)
B48–B51	1.760(5)	B49–B52	1.803(6)	B53–B53	1.948(8)
B48–B53	1.953(7)				
B–B bond lengths within the irregular polyhedron					
B54–B59	1.695(14)	B55–B58	1.913(16)	B57–B58	1.816(18)
B54–B55	1.819(13)	B56–B58	1.315(15)	B57–B59	1.840(25)
B54–B57	1.945(15)	B56–B59	1.810(22)	B58–B59	1.273(17)

Table 3 (continued)

B–B bond lengths within B <sub>12</sub> icosahedra					
B54–B58	1.985(11)	B56–B57	1.995(19)	B58–B58	1.734(23)
B55–B55	1.755(22)	B57–B59	1.103(25)	B59–B59	1.923(37)
B55–B59	1.830(21)	B57–B57	1.129(30)		
B–B bond lengths for linkages between polyhedron units					
B2–B9	1.734(9)	B16–B35	1.794(7)	B28–B43	1.687(9)
B3–B3	1.775(11)	B19–B49	1.758(7)	B33–B52	1.728(9)
B6–B51	1.766(6)	B20–B56	1.813(8)	B34–B40	1.657(6)
B7–B26	1.651(6)	B20–B58	1.818(12)	B36–B55	1.722(12)
B8–B44	1.716(6)	B/C21–B/C41	1.599(8)	B37–B37	1.860(13)
B11–B29	1.683(8)	B22–B32	1.662(9)	B/C38–B/C38	1.611(12)
B12–B47	1.690(10)	B23–B50	1.681(8)	B39–B54	1.667(12)
B13–B24	1.663(9)	B/C25–B/C25	1.619(12)		
B14–B42	1.686(9)	B27–B48	1.717(8)		
B–B bond lengths for linkages between bridge sites and units/other bridge sites					
B1–B68	1.790(7)	B17–B/C64	1.735(6)	B46–B65	1.787(8)
B4–B/C64	1.727(8)	B18–C60	1.602(7)	B53–B65	1.762(5)
B5–C63	1.629(5)	B30–B62	1.753(6)	B57–B66	1.805(16)
B10–B62	1.785(9)	B31–B/C67	1.701(8)	B62–B69	1.809(7)
B15–C63	1.629(8)	B45–B61	1.773(8)		

and the latter groups I4, I5 and I7 all of which include carbon atoms have 0.06–0.07 Å smaller values of 1.754, 1.763 and 1.755 Å, respectively. The intrapolyhedron bond distances of B<sub>9</sub> and B<sub>10</sub> polyhedra range from 1.755 to 1.924 Å and from 1.722 to 1.953 Å, respectively. Both have the same average value of 1.811 Å. Several bond distances within the irregular polyhedron are too short for both sites to be occupied simultaneously as mentioned above.

The interpolyhedron B–B bond distances range from 1.651 to 1.860 Å. The interpolyhedron B/C–B/C bond distances are much shorter and range from 1.599 to 1.619 Å. The B–B, B–C and B–B/C bond distances for linkages between bridge sites and polyhedron units/other bridge sites range from 1.753 to 1.809 Å, from 1.602 to 1.629 Å and from 1.701 to 1.735 Å, respectively, all of which are not so much different from the intericosahedron bond distances.

The interatomic Si–B and Sc–B distances are summarized in Table 4. Three B56 atoms surround Si1, where the bond distance is 1.883 Å. Three C63 atoms and one C60 atom tetrahedrally coordinate to Si2, where the Si2–C60 distance is about 0.1 Å shorter than the Si2–C63 distance. The Si2–C60 distance is comparable with the Si–C bond distance of 1.883 Å in SiC. The nearest neighbor distances of Sc–B are greater than 2.27 Å except for the Sc8–B57 and B58 distances of 1.974 Å. The distance is too short for both sites to be occupied simultaneously. Moreover the Sc8–Sc8 distance of 2.275 Å is also too short to be occupied simultaneously. Thus the site occupancies of all Sc8, B57 and B58 sites are roughly 50%.

## 2.2. Description of the structure

The crystal structure of Sc<sub>3.67–x</sub>B<sub>41.4–y–z</sub>C<sub>0.67+z</sub>Si<sub>0.33–w</sub> is characterized by a boron framework structure as usual boron-rich borides. In order to understand the framework structure it is convenient to extract some larger structure units consisting of several icosahedra. Thus three pillar-like structures that stand along *c*-axis were extracted from the boron framework structure. The first one consists of the icosahedra I1 and I3 and the irregularly shaped B<sub>16</sub> polyhedra as shown in Fig. 1. Its centerline parallel to the *c*-axis runs through the point (2/3, 1/3, 0). The top and bottom parts of the pillar like structure were constructed by the so-called super-octahedron. In the super-octahedron the central Si2 is tetrahedrally coordinated by three C60 and one C63 like a SiC<sub>4</sub> bonding unit in SiC. The tetrahedron is further octahedrally coordinated by three icosahedra I1 and three icosahedra I3. These icosahedra are bridged by three B64 and one B68. The same kind of super-octahedron has been found in the boron framework structure of the cubic phase Sc<sub>0.83–x</sub>B<sub>10.0–y</sub>C<sub>0.17+y</sub>Si<sub>0.083–z</sub> [4]. Si1 bridges three B<sub>16</sub> polyhedra through B56 at the top and bottom positions.

The second one whose centerline runs through the point (1/3, 2/3, 0) consists of the icosahedra I2, I5, and I6 and the B<sub>10</sub> polyhedron as shown in Fig. 2. Both are dominant structure units of the boron framework structure and the third one has a role to bridge both. The third one whose centerline runs through (0, 0, 0) consists of the icosahedra I7 and I4 and the polyhedra B<sub>9</sub> and B<sub>10</sub> as shown in Fig. 3. The B<sub>10</sub> polyhedra are

Table 4  
Interatomic Si–B and Sc–B distances (Å)

<i>Si–B/C distances</i>					
Si1–B56	1.883(13)	3	Si2–C60	1.889(12)	1
Si1–Sc8	2.481(4)	3	Si2–C63	1.985(6)	3
<i>Sc–B distances</i>					
Sc1–B65	2.421(6)	3	Sc2–B44	2.373(4)	4
Sc1–B50	2.455(6)	3	Sc2–B68	2.411(7)	2
Sc1–B53	2.563(4)	6	Sc2–B1	2.647(5)	4
			Sc2–B8	2.687(3)	2
Sc4–B/C64	2.362(5)	1	Sc5–B65	2.274(6)	1
Sc4–B49	2.395(5)	1	Sc5–C63	2.284(6)	1
Sc4–B51	2.450(4)	1	Sc5–B46	2.434(6)	1
Sc4–B62	2.493(5)	1	Sc5–B5	2.548(4)	2
Sc4–B52	2.508(5)	1	Sc5–B44	2.619(4)	2
Sc4–B47	2.537(5)	1	Sc5–B15	2.645(6)	1
Sc4–B10	2.597(5)	1	Sc5–B8	2.650(5)	2
Sc4–B30	2.627(4)	1	Sc5–B53	2.768(4)	2
Sc4–B17	2.659(5)	1			
Sc4–B33	2.661(4)	1			
Sc4–B12	2.682(4)	1			
Sc7–B55	2.534(11)	4	Sc8–B58	1.974(11)	2
Sc7–B/C67	2.567(8)	2	Sc8–B57	1.974(7)	2
Sc7–B36	2.714(5)	4	Sc8–Sc8	2.275(4)	1
			Sc8–B54	2.291(9)	2
			Sc8–B66	2.325(2)	1
			Sc8–B56	2.418(9)	2
			Sc8–B39	2.460(6)	2

Every third column indicates number of equivalent atoms.

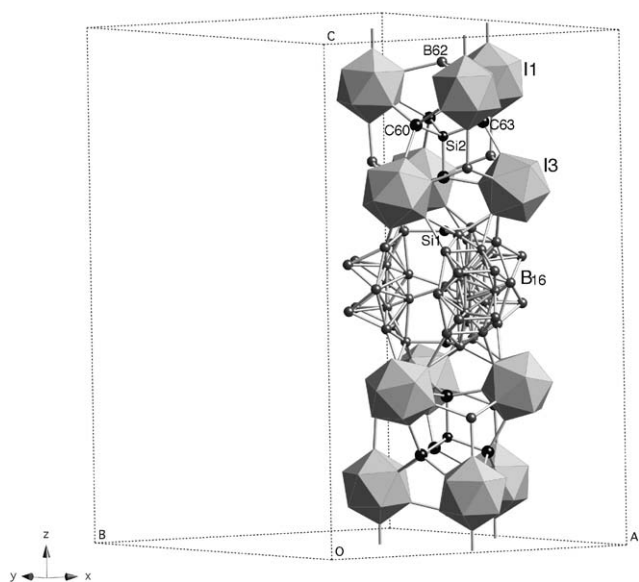


Fig. 1. The boron pillar-like structure unit whose central axis runs through the point  $(2/3, 1/3, 0)$  consists of the icosahedra I1, I3 and the irregularly shaped B<sub>16</sub> polyhedron.

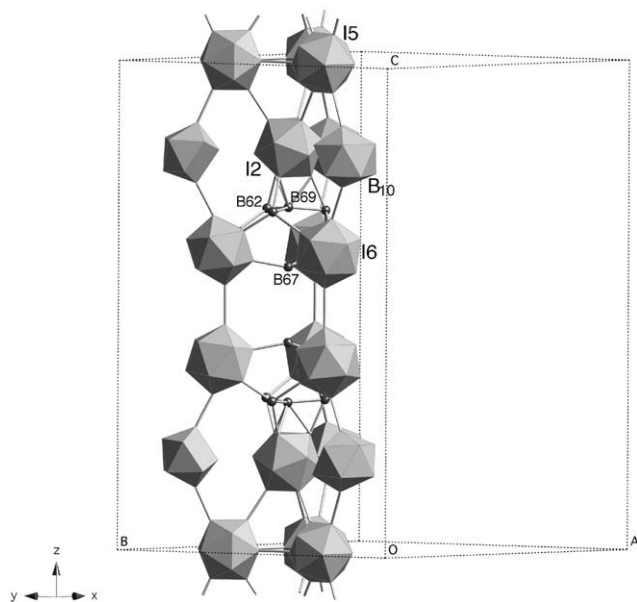


Fig. 2. The boron pillar-like structure unit whose central axis runs through the point  $(1/3, 2/3, 0)$  consists of the icosahedra I2, I5, I6 and the B<sub>10</sub> polyhedron.

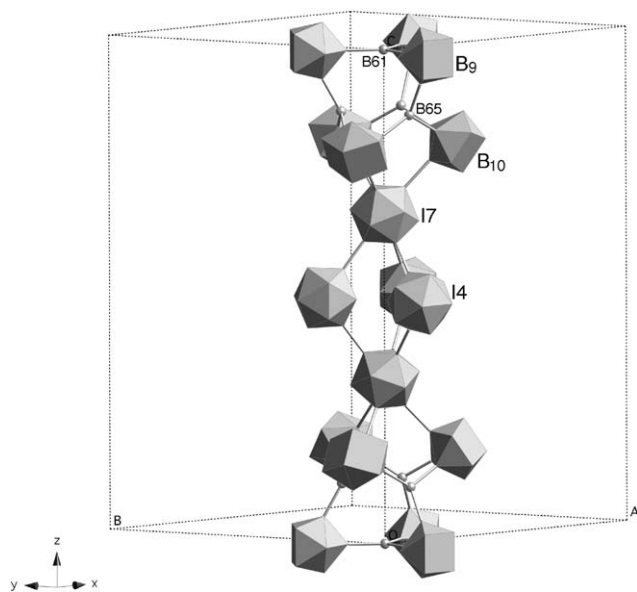


Fig. 3. The boron pillar-like structure unit whose central axis runs through the origin (0, 0, 0) consists of the icosahedra I4, I7, the  $B_9$  polyhedron and the  $B_{10}$  polyhedron.

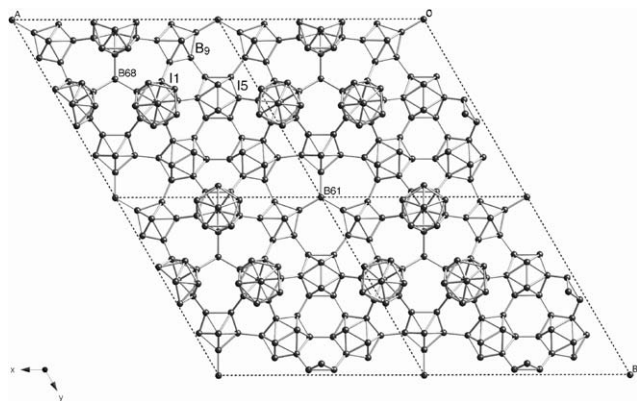


Fig. 4. The (001) boron network layer at  $z = 0$  depicted in a range  $0 < x < 2$ ,  $0 < y < 2$  and  $-0.2 < z < 0.2$ .

depicted in both second and third pillar-like structures as one of the constituents in order to understand the mutual relation easily.

One can understand easier such mutual relation between these three pillar-like structures by seeing a network linkage in the boron framework structure. Fig. 4 depicts a network linkage spanned at  $z = 0$  in a range  $0 < x < 2$ ,  $0 < y < 2$ ,  $-0.2 < z < 0.2$ . A triangle formed by three icosahedra I1 and the central B68 is the constituent of the first pillar-like structure. Another triangle formed by three icosahedra I5 is the constituent of the second pillar-like structure. The last triangle formed by three polyhedra  $B_9$  and the central B61 is the constituent of the third pillar-like structure.

The network linkage shown in Fig. 4 has another important meaning. The present hexagonal phase appeared as inclusions of the cubic phase single crystals

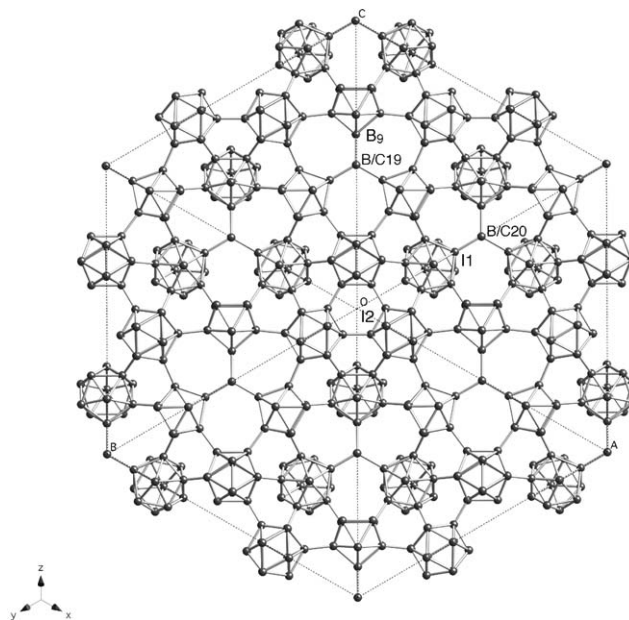


Fig. 5. The sliced (111) network structure of the cubic phase. The network structure coincides with the (001) network structure of the hexagonal phase shown in Fig. 4.

grown by the floating zone method as mentioned before; however, it looked like intergrowth. This suggested that some characteristic network structure in both crystal structures must have a similarity. It is reasonable to expect that such network structure in the cubic phase would occur in a slice parallel to the (111) plane. Fig. 5 shows the expected network structure in the cubic phase. A triangle formed by three icosahedra  $I1_{\text{cubic}}$  and the central  $B/C20_{\text{cubic}}$  corresponds to the first one for the hexagonal structure. Another triangle formed by three icosahedra  $I2_{\text{cubic}}$  corresponds to the second one. The last triangle formed by three  $B_9$  polyhedra and the central  $B/C19_{\text{cubic}}$  corresponds to the last one for the hexagonal structure. Both network structures are almost same, which allows the intergrowth of the hexagonal phase in the cubic phase.

Sc atoms reside in the voids of the boron framework structure. As shown in Fig. 6(a), Sc1 reside in a void of the third pillar-like structure surrounded by three  $B_{10}$  polyhedra, the icosahedron I4 and the bridging B65 atom. Sc2 occupies a void between the first and the third pillar-like structures surrounded by the  $B_9$  polyhedron, four icosahedra I1 and two bridge site B68 atoms as shown in Fig. 6(b). The environment of Sc3 is somehow similar to that of Sc1, which needs to incline the symmetry axis of the Sc1 environment more than  $90^\circ$  and to replace two of three  $B_{10}$  polyhedra to the  $B_9$  polyhedron as shown in Fig. 6(c). Two Sc4 sites in a mirror symmetry relation are depicted in Fig. 6(d), where Sc4 is surrounded by the icosahedra I1, I2, I3, I6, the  $B_{10}$  polyhedron and the bridging B62 and B64 atoms. The distance between neighboring Sc4 atoms is



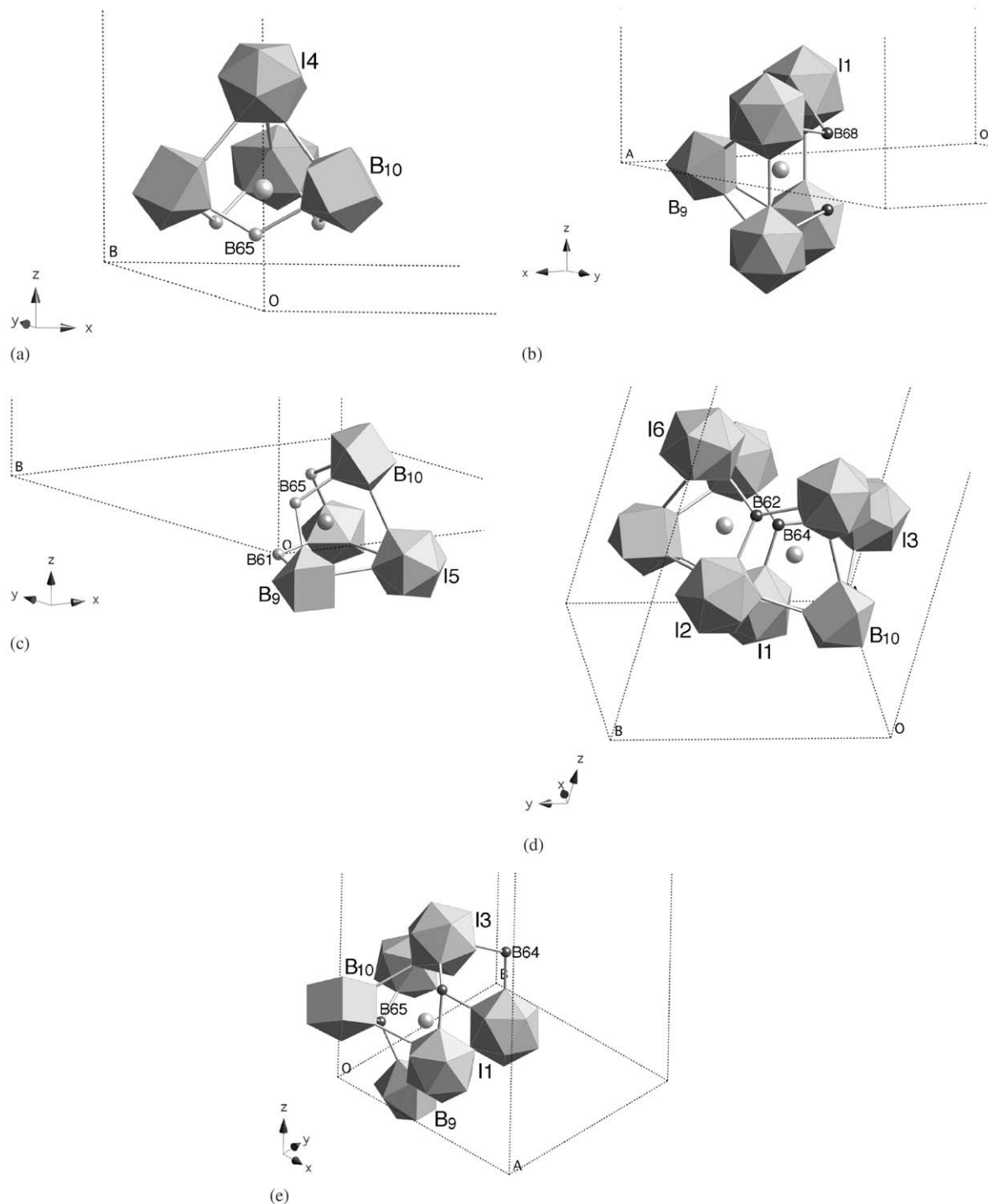


Fig. 6. Polyhedron environments of (a) the Sc1 atom, (b) the Sc2 atom, (c) the Sc3 atom, (d) the Sc4 atoms, (e) the Sc5 atom, (f) the Sc6 atom, (g) the Sc7 atoms and (h) the Sc8 atoms.

3.092 Å Fig. 6(e) shows the environment of Sc5 that is surrounded by two icosahedra I1, one icosahedron I3, two B<sub>10</sub> polyhedra, one B<sub>9</sub> polyhedron and the bridging two B/C64 and B65 atoms. The void for Sc5 opens between the first and the third pillar-like structures. Sc6 resides in a void between the first and the second pillar-

like structures surrounded by two icosahedra I3, two icosahedra I6, the bridging B62 and B/C64 atoms and a rectangular framework formed by two B55 and two B58 atoms as shown in Fig. 6(f). The occupancies of both B55 and B58 sites are only 87% and 44%, respectively, so that the rectangular framework is not always

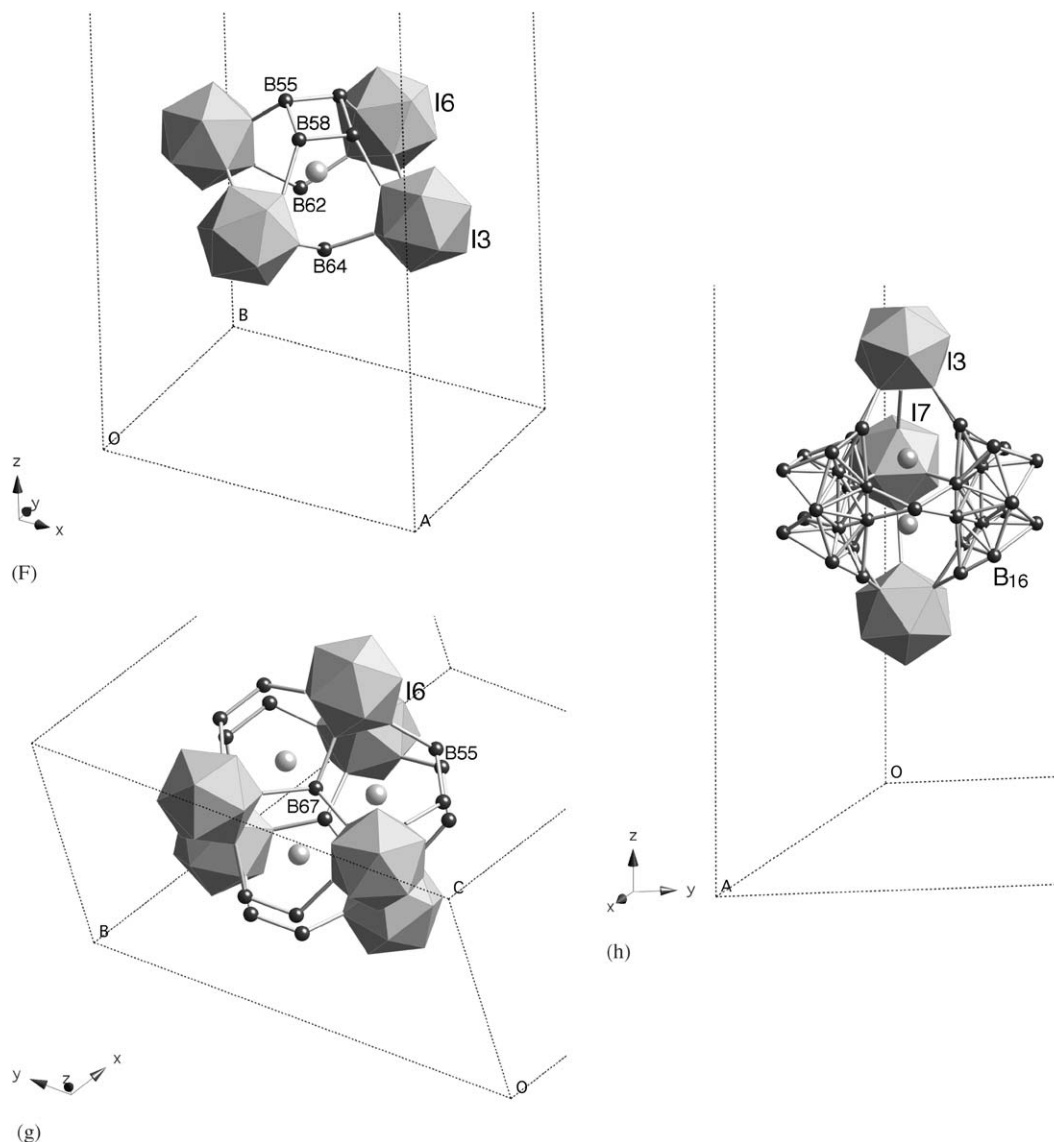


Fig. 6 (continued).

completed. Three Sc7 atoms form a triangle located in the second pillar-like structure as shown in Fig. 6(g). The distance between neighboring Sc7 atoms is 3.108 Å. Sc8 resides in a void of the first pillar-like structure surrounded by the icosahedra I3, I7 and the irregularly shaped B<sub>16</sub> polyhedra as shown in Fig. 6(h). The distance between a pair of the Sc8 sites in the figure is only 2.275 Å that is too short for the pair sites to be occupied simultaneously. Correspondingly the occupancy of the Sc8 site is 49%.

### 3. Concluding remarks

A novel compound Sc<sub>3.67-x</sub>B<sub>41.4-y-z</sub>C<sub>0.67+z</sub>Si<sub>0.33-w</sub> is established as a newly found quaternary Sc–B–C–Si

phase. Single crystal structure analysis revealed that the compound Sc<sub>3.67-x</sub>B<sub>41.4-y-z</sub>C<sub>0.67+z</sub>Si<sub>0.33-w</sub> has the hexagonal structure with lattice constants  $a = b = 1.43055(8)$  nm and  $c = 2.37477(13)$  nm and space group  $P\bar{6}m2$  (No. 187). There are 79 structurally independent atoms in the unit cell; eight partially occupied Sc sites, 62 B sites, two C sites, six B/C mixed occupancy sites and two Si sites. By most of these boron and carbon atoms seven structurally independent B<sub>12</sub> icosahedra, one B<sub>9</sub> polyhedron, one B<sub>10</sub> polyhedron and one irregularly shaped B<sub>16</sub> polyhedron in which only 10.7 boron atoms are available are formed. In order to describe the boron framework structure three pillar-like structure units were extracted. Sc atoms occupy the voids in the boron framework structure.

The previous cubic and orthorhombic phases could be synthesized as a ternary Sc–B–C compound, although Si addition was necessary for the floating zone crystal growth. The present hexagonal phase could not be synthesized as a ternary compound up to now. It is most likely to be a quaternary phase. Unfortunately the hexagonal phase was obtained only as a parasitic intergrowth phase in the cubic phase during the floating zone crystal growth. More careful examination of the phase relation between these phases may allow single-phase crystal growth of the hexagonal phase by the floating zone method.

### Acknowledgments

The authors thank Mr. K. Kosuda for EPMA measurements.

### References

- [1] T. Tanaka, Z.U. Rek, Joe Wong, M. Rowen, J. Crystal Growth 192 (1998) 141–151.
- [2] Joe Wong, T. Tanaka, M. Rowen, F. Schäfers, B.R. Müller, Z.U. Rek, J. Synchrotron Radiat. 6 (1999) 1086–1095.
- [3] Y. Shi, A. Leithe-Jasper, T. Tanaka, J. Solid State Chem. 148 (1999) 250–259.
- [4] T. Tanaka, A. Sato, J. Solid State Chem. 165 (2002) 148–158.
- [5] T. Tanaka, A. Yamamoto, A. Sato, J. Solid State Chem. 168 (2002) 192–201.
- [6] A. Altomare, G. Cascarano, C. Giacovazzo, A. Guagliardi, M. Burla, G. Polidori, M. Camalli, J. Appl. Crystallogr. 27 (1994) 435.
- [7] G.M. Sheldrick, SHELX97: a program for the solution and refinement of crystal structures, Universität Göttingen, Göttingen, Germany, 1997.
- [8] D. Palmer, CrystalMaker, Version 5.0.7, CrystalMaker Software, Bicester, Oxfordshire, OX6 7BS, UK.
- [9] I. Higashi, K. Kobayashi, T. Tanaka, Y. Ishizawa, J. Solid State Chem. 133 (1997) 16–20.